Eur. Phys. J. B **51**, 389–393 (2006)
DOI: 10.1140/epjb/e2006-00224-8

THE EUROPEAN PHYSICAL JOURNAL B

Spiral tip meandering induced by excitability modulation

X. Zhang[1] and G. Hu[1,2,a]

[1] Department of Physics, Beijing Normal University, Beijing 100875, P.R. China
[2] Chinese Center for Advanced Science and Technology (World Laboratory), Beijing 8730, P.R. China

Received 31 January 2006 / Received in final form 27 March 2006
Published online 13 June 2006 –

Abstract. In this work, we introduce a spatiotemporal modulation for excitability into an excitable medium, the Barkley model. The modulation can make the spiral wave tip meandering. Various types of periodic spiral and quasiperiodic meandering spiral motions can be observed numerically by varying the modulation. And the theoretical analysis for the conditions of Hopf bifurcation, based on an ordinary-differential-equation (ODE) model, is applied to well explain the rich behaviors of numerical simulations.

PACS. 82.40.Ck Pattern formation in reactions with diffusion, flow and heat transfer

1 Introduction

Spiral waves constitute an example of self-organizing activity that have been observed in various excitable media such as Belousov-Zhabotinsky reactions [1,2], cardiac muscles [3] and neural networks [4]. One common feature of these waves is their tendency to meander [5–8]. Under some conditions, the spiral tip does not trace out a periodic circle, but instead follows a more complicated quasiperiodic flower-shape trajectory, which may be epicycloid, cycloidal, hypocycloid, and even random walk over long timescales [9]. In the past few years, controlling the motions of spiral waves has attracted much interest [10–17]. Some researches aim at changing the dynamics of spiral waves by applying certain kind of controlling scheme to the system variables. For example, with modulation of the global feedback signals, the dynamical behavior of spiral waves can be essentially changed [10]. Alternatively, both constant and periodic electric fields imposed on the excitable media can both produce spiral wave drift [11,12], while the spiral tip can even be attracted by the localized small-world connections in excitable systems [13]. Others aim at controlling the spiral dynamics by modulating one of the system parameters. With periodic sinusoidal signals, resonance drifts and entrainment bands are observed in excitable media [14,15]. Applying feedback controlling signals can also force the spiral tip execute a circular trajectory [16,17]. It has been shown that there are two vital independent parameters of excitable media, the excitation threshold and the ratio of characteristic rates of recovery and excitation, which determine the excitability above the threshold. However, until now, most of the parametric modulating methods are carried out through the former parameters and the investigation of possible modulation of the latter parameter has been much less [14–17]. This motivates us to investigate the spiral dynamics under the modulation of the ratio of characteristic rates of recovery and excitation of the excitability of the medium, which is of crucial importance and of system evolution dependence in general.

In this paper, we use the spatiotemporal force to modulate the ratio of characteristic rates of recovery and excitation of the excitability of the medium, which determine the excitability of the media above the excitation threshold. The modulation can make the spiral tip meandering, including inward-petal and outward-petal meandering, as well as linear drift. In addition, we find that the modulation mechanism can be interpreted by adding a similar driving item to the ODE model [8,18]. The theoretical predictions of the simplified ODE model system are consistent with our numerical simulations in demonstrating rich bifurcations to various meandering states.

2 Model with excitability modulation and numerical simulations of meandering trajectories

We introduce a spatiotemporal driving force for the parameter ϵ, which determines the excitability above the threshold, into the Barkley Model [19]:

$$\frac{\partial u}{\partial t} = \frac{1}{\epsilon + E} u(1-u)(u - \frac{v-b}{a}) + \nabla^2 u$$
$$\frac{\partial v}{\partial t} = u - v \qquad (1)$$

[a] e-mail: ganghu@bnu.edu.cn

where $a = 0.8,\ b = 0.05,\ \epsilon = 0.02$, under these conditions, equations (1) have a rigidly rotating spiral wave solution at $E = 0$. The driving term is

$$E = \begin{cases} 0 & t \le t_0 \\ \dfrac{\gamma_1 v}{\gamma_2 + u} & t > t_0. \end{cases} \quad (2)$$

In equation (2), t_0 stands for the long transient time, which means that the driving force E dose not work until equations (1) have a periodic spiral solution ($t > t_0$). It is obvious that the driving force is zero at the steady state ($u = v = 0$), and the excitability modulation functions effectively where the variable states are excited ($u > 0, v > 0$). The spatiotemporal modulation term equation (2) adopted here is based on the fact that the excitability in a reaction diffusion system may be spatially inhomogeneous and the evolution of the system is generally expected to influence the excitability. The reasons why we choose the particular modulation form are twofold. On one hand, the form of equation (2) is very simple. On the other hand, most importantly, this modulation form has some possibly practical implications in describing cardiac systems, which has been used to a cardiac cell model [20] (i.e. AP model) in order to recover approximately the actual cardiac-cell restitution curve with considerably simplified dynamic equations.

In the next section, we conduct numerical simulations of equations (1), which are undertaken with zero flux boundary conditions. Laplacian operator is discretisized on a 240×240 lattice. The space step on the x and y directions are both equal to $h = 0.4$. This diffusion term are time stepped by the second-order Runge-Kutta method with time step $\tau = 0.02$. We take the spiral tip to be the intersection of two contours, $u = 0.5$ and $v = 0.5a - b$.

When $\gamma_1 = 0$, which means no driving force added, equations (1) have a periodic spiral. The corresponding tip trajectory is a circle, as shown in Figure 1a. When $\gamma_1 \neq 0$, with excitability modulation, the spiral wave tip leaves its previous circle trajectory and undergoes various bifurcations to different types of meandering motions. For simplicity, we fix the parameter $\gamma_2 = 1.0$ and change parameter γ_1 only for studying variation of the tip motions.

At $\gamma_1 = 0.1$, the meandering tip has an outward-petal (hypocycloid) trajectory, as shown in Figure 1b. For $\gamma_1 = 0.154$, the tip is subject to linear drift demonstrated in Figure 1c. With $\gamma_1 = 0.18$, the meandering tip trajectory becomes an inward-petal (epicycloid) orbit, plotted in Figure 1d. Increasing γ_1 up to $\gamma_1 = 0.26$, the tip is eventually driven from its original circle(i.e. the circle of Fig. 1a) to another circle trajectory, as shown in Figure 1e.

For having a global view of the distributions of different patterns in the parameter (γ_1, γ_2) plane, we plot the phase diagram in Figure 2, in which, from the up-left side to the bottom-right side, the tip motion varies from stationary state (Region I, $u = v = 0$), to periodic circle (Region II), to quausiperiodic inward-petal meandering (Region III), to linear drift (Region IV, a single line region), to outward-petal meandering (Region V), and finally to periodic circle motion again (Region VI). Note, the circle orbit in Region II is different from that of Figure 1a in Region VI with both location and circle radius.

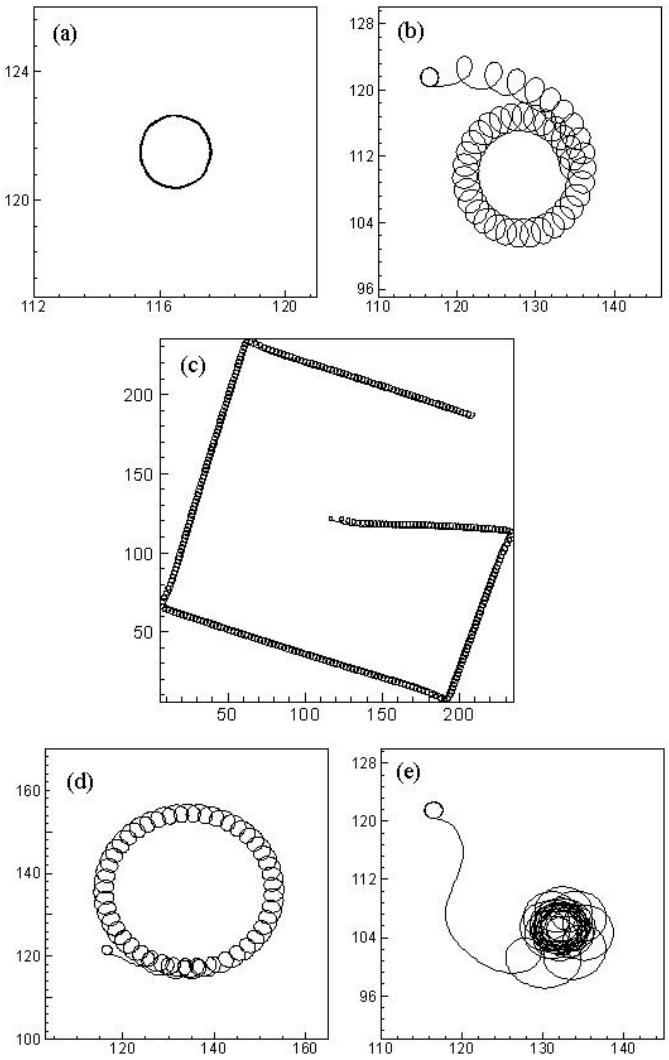

Fig. 1. Tip trajectories under different driving forces with the conditions of $a = 0.8,\ b = 0.05,\ \epsilon = 0.02,\ \gamma_2 = 1.0$ in equations (1). The little circle in (b)–(e) is the original circular tip trajectory when $t \le t_0$. (a) $\gamma_1 = 0.0$, (b) $\gamma_1 = 0.1$, (c) $\gamma_1 = 0.154$, (d) $\gamma_1 = 0.18$, (e) $\gamma_1 = 0.26$.

The mechanisms underlying the meandering behaviors caused by the excitability modulation can be intuitively understood as following. Because of the existence of parameter ϵ, the refractory variable v always lags behind the active variable u in equations (1). The added driving item $E = \frac{\gamma_1 v}{\gamma_2 + u}$ will bring in a gradient distribution of excitability along the normal direction of the spiral arm that makes the excitability of the wave front of spiral greater than the wave back. The weak excitability on the wave back then makes the corresponding cells more difficult to be refractory and cause the separation of wave front and wave back. The curvature near the spiral tip then decreases. According to the eikonal relation in an excitable medium [21], this curvature decrease leads to that the increase of the normal velocity of wave front near the spiral tip. Hence,

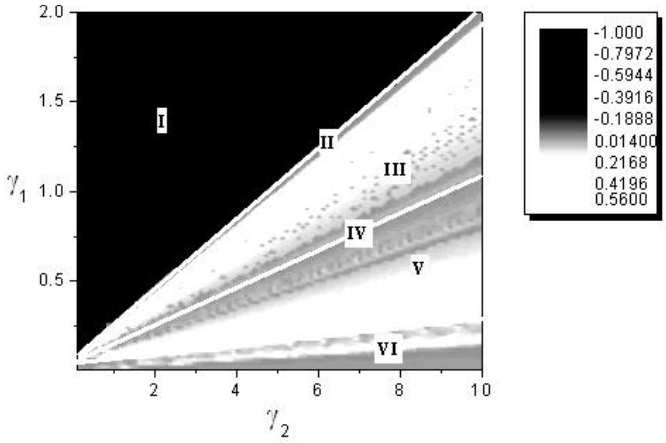

Fig. 2. Phase diagram in parameter plane (γ_1, γ_2) of equations (1). The gray depth is determined by r_2/r_1 with r_1 being the radius of secondary circle in the laboratory frame and r_2 being the radius of the elementary circle in the rotating frame. For the homogeneous steady state of equations (1), we set $r_2/r_1 = -1$. Six different regions are classified as: I steady state; II and VI Periodic spirals; III Epicycloid spirals (inward-petal meandering); IV line drift spirals; V Hypocycloid spirals (outward-petal meandering).

the spiral tip cannot follow its original circular trajectory any longer and begins to meander.

Meandering appears from periodic circle as the cause of the supercritical Hopf bifurcation [22] that introduces the second frequency into the basic system. Therefore, there are two frequencies exist in the meandering solutions: one is the original frequency ω_1 of the periodic spiral, the other is ω_2 introduced by the Hopf bifurcation. The spiral tip will perform a quasiperiodic flower-shape motion. When the two frequencies equal to each other (on the Region IV, in Fig. 2), the tip has linear drift trajectory. From Figure 2, we can also find the different kinds of meandering motions, one with inward petals (Region III, $\omega_1 > \omega_2$) and the other with outward petals (Region V, $\omega_1 < \omega_2$). It is easy to understand that as the driving force is sufficiently large (large γ_1), the excitability of the system becomes so weak that it no longer sustains any spiral. The whole system thus comes into the steady state (Region I). On the other hand, when the driving force is small, Hopf bifurcation cannot happen. The spiral tip can only keep its circular periodic trajectory (Region VI).

3 Theoretical analysis based on the ODE model

Apart from the above intuitive understanding of the excitability modulation inducing meandering, we can further study the effects of the excitability modulation in a more analytical (though approximate) manner. We utilize the ODE model [8,18] and bring certain driving force into this model. If the tip motion of the ODE model system agrees with the results of direct numerical simulations of the reaction diffusion system equations (1) qualitatively, we conclude that the added force in the ODE system has attacked the essence of the excitability modulation.

The transition from rigidly rotating spiral to meandering spirals is known as an epicycle motion superimposed on the basic spiral wave circle. Barkley first gave the explanation of the resonant meandering and revealed the Hopf bifurcation from the steady state (rigidly rotating spirals) to the quasiperiodic meandering state. And he proposed a low-dimensional, weakly nonlinear ordinary-differential-equation (ODE) model [8,18] to describe the Hopf bifurcation dynamics in the vicinity of such a codimension-two point. This ODE model is invariant under a representation of distance-preserving transformations of the plane (rotations, reflections, and translations) and has rotating-wave solutions which undergo a Hopf bifurcation. The simplest form satisfying all the above symmetries reads (Eqs. (3) in Ref. [8])

$$\begin{aligned} \dot{x} &= s\cos\phi \\ \dot{y} &= s\sin\phi \\ \dot{\phi} &= w \cdot h(s^2, w^2) \\ \dot{s} &= s \cdot f(s^2, w^2) \\ \dot{w} &= w \cdot g(s^2, w^2). \end{aligned} \tag{3}$$

Where *f,* g and h have the expression:

$$\begin{aligned} f(s^2, w^2) &= \alpha_0 + \alpha_1 s^2 + \alpha_2 w^2 - s^4 \\ g(s^2, w^2) &= \beta_1 s^2 - w^2 - 1 \\ h(s^2, w^2) &= \gamma_0. \end{aligned} \tag{4}$$

Following Barkley's analysis, we simply take $\alpha_0 = -0.25,\ \alpha_1 = 7.0,\ \alpha_2 = -5.0,\ \beta_1 = 1.0,\ \gamma_0 = \sqrt{28}$, fitting the results of the original Barkley model without modulation (i.e. $E = 0$ in Eqs. (1)) [8,18]. Under these conditions, the trajectory of equations (3) in the phase space (x, y) is a circle, which stands for a rigidly rotating spiral wave in a real reaction diffusion system.

Basing on the analytic methods in reference [18], we use $p = s^2,\ p \in \mathbb{R}$ and $q = w^2, q \in \mathbb{R}$, and rewrite equations (3) as:

$$\begin{aligned} \dot{p} &= 2p \cdot f(p, q) \\ \dot{q} &= 2q \cdot g(p, q) \\ f(p, q) &= -\frac{1}{4} + 7p - 5q - p^2 \\ g(p, q) &= p - q - 1. \end{aligned} \tag{5}$$

Up to now the formulas are generally valid for describing the tip motion in excitable media. Now we add the excitability modulation to equations (5). There is no exact derivation specifying the modulation term in the ODE (5) from the original PDE (1) and (2). We test this modulation according to the requirements of simplicity, and fitting of results of both the original PDE and the reduced ODE. We try an ODE with modulation as

$$\begin{aligned} \dot{p} &= 2p \cdot \left[f(p, q) + \frac{\mu_1 p}{\mu_2 + q} \right] \\ \dot{q} &= 2q \cdot g(p, q) \end{aligned} \tag{6}$$

where μ_1 and μ_2 in equations (6) qualitatively correspond to the parameters γ_1 and γ_2 in equations (1), respectively. We now analyze equations.(6) for searching conditions of the Hopf bifurcation, which is the cause of tip meandering from its original circle trajectory, and compare the results of equations (6) with the numerical simulations of equations (1) and (2).

One of the steady state of equations (6) is $p = q = 0$, which means the homogeneous rest state in the original reaction diffusion system and we don't care about. The other solution can be solved from equations $f = g = 0$:

$$\begin{cases} -\frac{1}{4} + 7p - 5q - p^2 + \frac{\mu_1 p}{\mu_2 + q} = 0 \\ q = p - 1. \end{cases} \tag{7}$$

According to equations (7), the condition for the existence of rigidly rotating($q \neq 0$) is:

$$\mu_1 > -5.75\mu_2. \tag{8}$$

Now we solve equations (7) and abandon the complex roots which disagree with our basic assumptions, $p \in \mathbb{R}$ and $q \in \mathbb{R}$, and thus obtain

$$\begin{cases} p_0 = \frac{W}{6} + \frac{1}{W}(+2\mu_1 + \frac{23}{2} + \frac{2}{3}\mu_2^2) - \frac{1}{3}\mu_2 + 1 \\ q_0 = p_0 - 1, \end{cases} \tag{9}$$

where

$$W = -36\mu_1\mu_2 + 414\mu_2 + 108\mu_1 - 8\mu_2^3 + 3\left(\begin{array}{c} -36501 + 12696\mu_2^2 - 19044\mu_1 - 1104\mu_2^4 \\ -5520\mu_2^2\mu_1 - 2016\mu_1^2 - 48\mu_2^2\mu_1^2 - 192\mu_1^3 \\ -192\mu_2^3\mu_1 + 9936\mu_1\mu_2 - 864\mu_1^2\mu_2 \end{array}\right)^{\frac{1}{3}}.$$

The conditions of Hopf bifurcation can be computed by linear stability analyse of equations (6). The Jacobian Matrix at the steady state (p_0, q_0) is:

$$J = \begin{pmatrix} 2p_0\left(7 - 2p_0 + \frac{\mu_1}{\mu_2 + q_0}\right) & 2p_0\left(-5 - \frac{\mu_1 p_0}{(\mu_2 + q_0)^2}\right) \\ 2q_0 & 2p_0 - 4q_0 - 2 \end{pmatrix}. \tag{10}$$

On the Hopf bifurcation point, the trace and the determinant of matrix J satisfy:

$$tr = \frac{4p_0^3 + (4\mu_2 - 16)p_0^2 - (2\mu_1 + 12\mu_2 - 10p_0)p_0 - 2\mu_2 + 2}{\mu_2 + p_0 - 1} = 0 \tag{11a}$$

$$det = \frac{4p_0\left(\begin{array}{c} 2p_0^4 + (-8 + 4\mu_2)p_0^3 + (12 + 2\mu_2^2 - 12\mu_2)p_0^2 + \\ (-8 + 12\mu_2 - 4\mu_2^2 + \mu_1 - \mu_1\mu_2)p_0 + \\ \mu_1\mu_2 - 4\mu_2 + 2 - \mu_1 + 2\mu_2^2 \end{array}\right)}{(\mu_2 + p_0 - 1)^2} > 0. \tag{11b}$$

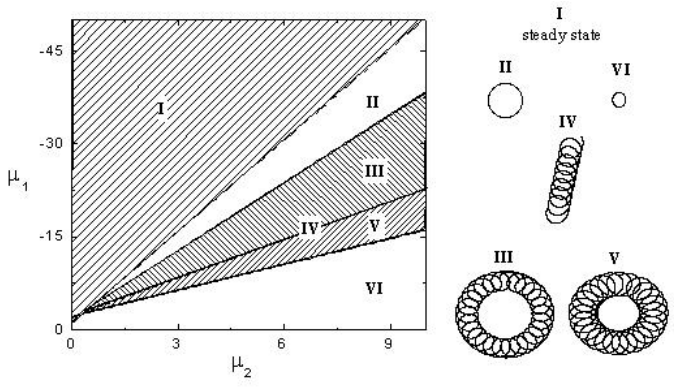

Fig. 3. Phase diagram in parameter space (μ_1, μ_2) of the modulated ODE model (6). All the index numbers have exactly the same meanings as Figure 2. The four borderlines between the adjacent regions correspond to: equation (8) (the line between Region I and II), equations (12a) (the line between Region II and III), Region IV (the line between between Region III and Region V) that is computed numerically and equations (12b) (the line between Region V and VI).

The condition for Hopf bifurcation is determined by equations (11). Given the steady state (p_0, q_0), we have the critical borders of Hopf bifurcation:

$$\mu_1 = -\frac{11}{6}(1 + 2\mu_2) \tag{12a}$$

$$\mu_1 = -\frac{7}{10}(3 + 2\mu_2). \tag{12b}$$

From equations (8) and (12a), we can portrait the phase diagram of the solution of the modulated ODE model in the parameter space (μ_1, μ_2), as shown in Figure 3. By numerically computing the ODE system equations (3) and (6), we can distinguish six different regions with four borderlines in the parameter plane: I: steady state; II and VI: Periodic spirals; III: Epicycloid spirals (inward-petal meandering); IV: linear drift spirals; V: Hypocycloid spirals (outward-petal meandering). The four borderlines between the adjacent regions correspond to: equation (8) (the line between Region I and II); equations (12a) (the line between Region II and III); Region IV (the line between Region III and Region V) and equations (12b) (the line between Region V and VI). Region IV is computed numerically which cannot be given analytically because it is far from the Hopf bifurcation point.

Comparing Figures 2 and 3, it is obvious that the qualitative features of the original reaction-diffusion equations equations (1) are satisfactorily revealed by the simplified ordinary-differential-equation model equations (6). It means that the excitability modulation for parameter ϵ can effectively cause the Hopf bifurcation of the original steady periodic spirals solutions and make the spiral tip meandering.

4 Concluding remarks

In conclusion, we have introduced an spatiotemporal modulation for the excitability of reaction diffusion system of Barkley model, which can make the spiral wave tip meandering, including inward-petal and outward-petal meandering, as well as linear drift. The theoretical analysis based on the ODE model coincides very well with what we obtain in the original excitable media.

This work is supported by National 973 project of Nonlinear Science and the National Science Foundation of China (Grant Nos. 10335010).

References

1. Q. Ouyang, J.M. Flesselles, Nature **379**, 143 (1996)
2. A.L. Lin, M. Bertram, K. Martinez, H.L. Swinney, Phys. Rev. Lett. **84**, 4240 (2000)
3. Z.L. Qu, J. Kil, F.G. Xie, A. Garfinkel, J.N. Weiss, Biophys. J. **78**, 2761 (2000)
4. V.I. Sbitnev, Int. J. Bifurcation and Chaos **8**, 2341 (1998)
5. A.T. Winfree, Science **181**, 937 (1973)
6. A.T. Winfree, Chaos **1**, 303 (1991)
7. G. Li, Q. Ouyang, V. Petrov, H.L. Swinney, Phys. Rev. Lett. **77**, 2105 (1996)
8. D. Barkley, Phys. Rev. Lett. **72**, 164 (1994)
9. V.N. Biktashev, A.V. Holden, Physica D **116**, 342 (1998)
10. V.S. Zykov, H. Engel, Phys. Rev. E **66**, 016206 (2002)
11. V. Krinsky, E. Hamm, V. Voignier, Phys. Rev. Lett. **76**, 3854 (1996)
12. H. Zhang, B.B. Hu, G. Hu, J.H. Xiao, J. Chem. Phys. **119**, 4468 (2003)
13. X.N. Wang, Y. Lu, M.X. Jiang, Q. Ouyang, Phys. Rev. E **69**, 056223 (2004)
14. R. Mantel, D. Barkley, Phys. Rev. E **54**, 4791 (1996)
15. A. Schrader, M. Braune, H. Engel, Phys. Rev. E **52**, 98 (1995)
16. A. Karma, V.S. Zykov, Phys. Rev. Lett. **83**, 2453 (1999)
17. O. Kheowan, S. Kantrasiri, P. Wilairat, Phys. Rev. E **70**, 046221 (2004)
18. D. Barkley, I.G. Kevrekidis, Chaos **4**, 453 (1994)
19. D. Barkley, M. Kness, L.S. Tuckerman, Phys. Rev. A **42**, 2489 (1990)
20. R.R. Aliev, A.V. Panfilov, Chaos Solitons & Fractals **7**, 293 (1996)
21. A.M. Pertsov, M. Wellner, J. Jalife, Phys. Rev. Lett. **78**, 2656 (1997)
22. D. Barkley, Phys. Rev. Lett. **68**, 2090 (1992)